EXPERIMENTAL CHARACTERIZATION OF A MIMO UNDERGROUND MINE CHANNEL AT 2.45 GHz

Yacouba Coulibaly[1], Bilel Mnasri[1], Mourad Nedil[1, *], Ismail B. Mabrouk[2], Larbi Talbi[2], and Tayeb A. Denidni[3]

[1]University of Quebec at Abitibi-Témiscamingue, Canada

[2]University of Quebec at Outaouais, Pavillon Lucien-Brault, Canada

[3]INRS-EMT, Place Bonaventure 800, Canada

Abstract—In this paper, an experimental characterization of a MIMO underground channel is presented. A simple statistical model is proposed at 2.45 GHz. The channel is characterized in terms of path loss, shadowing, RMS delay spread, and capacity. The measurements are carried out in an underground mine, which is a harsh confined environment. The path loss model is extracted from measured data for the line of sight (LOS) and non-line of sight (NLOS) scenarios for both MIMO and SISO channels. The path loss exponent in LOS is less than 2 in MIMO and SISO as the environment has a dense concentration of scatterers. A statistical study is carried out to find the delay spread. For MIMO and SISO, there is no relation between the delay spread and the transmitter receiver distance. Furthermore, the delay spread of the MIMO is less than the one of the SISO channel in the LOS measurement campaigns. Aikake information criteria are used as a goodness of fit for different statistical distributions to represent the delay spread. According to the calculated capacity for a constant signal to noise ratio in LOS case, the transmission performance is significantly improved by using the MIMO scheme over the traditional SISO. Therefore, MIMO is an ideal candidate for future wireless underground communications.

1. INTRODUCTION

Recent advances in wireless communication systems require the propagation channel to be correctly characterized or modeled. This characterization is important as it provides a better understanding of propagation phenomena, such as reflection, diffusion and refraction, in any given environment. In a practical perspective, it enables engineers to design low cost, high performance and more efficient communication systems. Mines are rich in multipath components. Therefore, an accurate channel model is needed for the deployment of wireless communication in these confined environments [1–3]. Wired communication through leaky feeder or fiber optics and wireless communication are the different ways to transmit information in an underground mine. Compared to wired systems, wireless communications can be deployed anywhere in a mine, can withstand during disasters, and can offer low cost solutions. Wireless technology is used in the mining industry to improve the production through automation, to increase the safety, to reduce the maintenance cost and to allow the transfer of voice, data and video, in any remote location of the mine [1–4]. The demand for these high data rates has led to different potential viable solutions for wire-less communications. Using MIMO (multiple-input multiple-output) techniques [5–9] and ultra wideband techniques are two of the most important proposed schemes [10].

MIMO technology offers some advantages over SISO (Single-Input-Single-Output) [5–9]. The capacity is increased without an increase of the transmitted power. Better transmission quality and better communication coverage are achieved. Compared to the SISO system, the channel capacity of MIMO has significantly increased. The additional channel capacity can be used to improve the information transmission rate as well as the reliability of trans-mission communication system by increasing the information redundancy. Therefore, a number of research activities have been carried out for the study and evaluation of MIMO systems in various environments [5–9]. Underground mine, with high multipath components, are different from those environments considered previously [3, 4]. To date, very little attention has been given to the potential application of MIMO in underground mining environments, even though some examples have been proposed in different confined surroundings [11–15]. An experimental campaign is proposed in the C-band in a subway tunnel [11]. It is demonstrated that the irregularities in the tunnel can enhance the capacity of antennas with the same polarization. Spatial and polarization diversity are efficient for MIMO when the cross section

of the tunnel is rectangular. Sun and Akyildiz have shown through simulation that the optimal antenna can be designed in order to improve the capacity of empty tunnel and tunnel with obstruction [12]. Lienard et al. have carried out some measurements in a railway tunnel to increase the capacity of the transmission channel. They found out that the antennas alignment is an important parameter. For a constant SNR of 10 dB, the capacity of a SISO and a 4×4 MIMO are 3 bits/s/Hz and 8 bits/s/Hz, respectively [13]. A modal theory is used to analyze the MIMO wireless channel. With the help of a parametric study, the authors have demonstrated that the correlation between the transmitting and receiving antennas and the active mode number are critical [14]. A capacity of 3 bits/s/Hz with a SNR of 10 dB was also achieved. Finally, a MIMO channel with polarization diversity was characterized [15]. According to all these works, the capacity of an underground channel can be improved by using a MIMO scheme.

The objective of this paper is to characterize a MIMO underground mine channel and present statistical models. An accurate characterization and modeling can yield valuable information to the wireless communication engineers. With the obtained channel parameters, an efficient communication system can thereby be designed. The analysis is based on MIMO channel measurements at 2.45 GHz. For the purpose of comparison, SISO measurement campaigns were also conducted. This paper is organized as follows. Section 2 gives a brief description of the underground mine environment and the measurements procedure. Section 3 presents the experimental data where the path loss models, delay spread, and capacity of the channel were evaluated. Section 4, concludes the results of this study.

2. MEASUREMENT ENVIRONMENT

The measurements were performed in CANMET (Canadian Center for Minerals and Energy Technology), which is a government own experimental mine in Val d'Or, Canada. It is an old gold mine used to train miners or perform different type of experiments. The mine has many galleries, corridors, curves and first aid stations. The experimental campaign was conducted at a depth of 40 m. The ground is not even at many places as there are some bumps, ditches and water puddles. The lateral walls of the mine are not aligned. The width and the length are about 4 m to 5 m and 80 m, respectively. Different cables ranging from leaky feeder to fiber optics are present on the top of the ceiling. Fig. 1 shows an example of gallery of the underground mine.

Figure 1. A gallery of the underground mine.

3. MEASUREMENT SETUP AND PROCEDURE

As shown in Fig. 2, the measurement setup consists of a vector network analyzer (VNA), a power amplifier (PA), a low noise amplifier (LNA), two sets of switches, long low loss cables and antennas. The agilent E8363 VNA is used as both a transmitter and a receiver in the system. It measured the frequency transfer function with 1601 stepped frequency points in the range of 2 GHz to 3 GHz. The frequency spacing is 156.25 kHz, which correspond to time domain duration of 6400 ns. Therefore, the measurement system is capable of catching multipath components arriving with a delay up to 6400 ns.

This time duration of impulse response is found to be long for underground environment. The transmit power of the VNA was set to 10 dBm. The transmitted signal is amplified by a power amplifier NARDA of gain 30 dB, and fed to the antennas through some low loss cables. The receiving antennas are each connected to one output port of the switch. The received signal is then fed to the VNA through a RLNA low noise amplifier (LNA) of gain 30 dB in order to reduce the noise figure. The unused port of the switches antennas are automatically connected to 50 Ω loads. Four Cisco Aironet Very Short 2.4 GHz Omnidirectional monopole antennas (AIR-ANT2422SDW-R) are used. Their operating frequency range is from 2.4 GHz to 2.5 GHz. The 3 dB beamwidths in the azimuth and elevation plane are 360 degrees (Omnidi-rectional) and 50 degrees, respectively. A laser beam has been used to fix the height of the antennas from ground at 1 m. All antennas are vertically polarized and provide a gain of 2.5 dBi in the operational frequency band. For MIMO, the distance between the antennas is fixed at $\lambda/2$ at the frequency of 2.45 GHz.
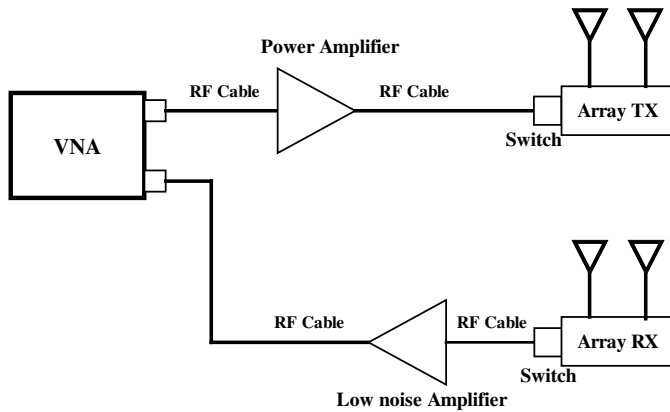
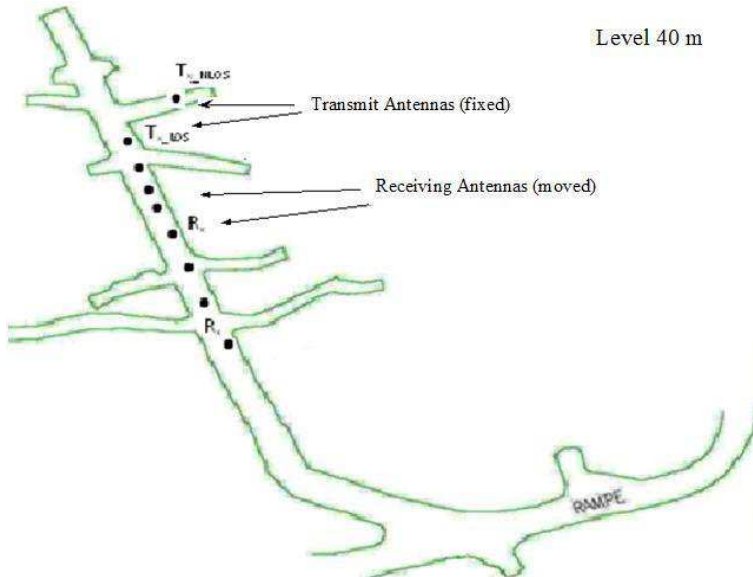**Figure 2.** Measurement setup.

Figure 3. Map of the gallery.

Before starting the measurements, a classical calibration of the VNA is done using the standard techniques. Then, a reference measurement is performed with the transmitting antenna and receiving antenna apart with 1 m separation distance. By doing this second calibration, the impairment effects of the LNA, the PA, the cables, connectors and antennas are removed. To characterize the propagation

channel in small scale, in the case of SISO, the receiver is moved on a grid square with 25 points (5×5) where the distance between each adjacent point is equal to 6.1 cm, which is $\lambda/2$ at the frequency of the 2.45 GHz. In the case of the MIMO, ten consecutive sweeps were averaged at each distance to obtain an important statistical data of the channel and to also reduce the effects of random noise. All measurement are done in the middle of the gallery. For MIMO and SISO, LOS and NLOS measurement scenarios were considered. As shown in Fig. 3, measurements were taken for a transmitter-receiver distance of 1 m to 26 m with a step of 1 m for LOS. For NLOS, the transmitter-receiver varied from 6 m to 26 m with the same step of 1 m. All measurements were performed with minimal human movement and activity. Therefore, the channel was considered stationary.

4. PATH LOSS

In the underground mine, the path loss of electromagnetic waves influences the received power and link budget of the system. In addition, it can provide important information that enables the proper design of communication systems. The average path loss can be deduced from the measurements using [16]:

$$PL(d)_{\mathrm{dB}} = \frac{1}{MN} \sum_{i=1}^{M} \sum_{j=1}^{M} |f(i,j,d)|^2 \qquad (1)$$

where $|f(i,j,d)|$ is the measured complex frequency response deduced from the time domain response through an inverse Fourier transform. M and N are the number of data points (which is 1601), the numbers of local sweeps, respectively. In the case of the MIMO channel, the mean path loss for the MIMO links can be averaged, as these channels are not so different from one another.

It is well known that the path loss depends on the distance. The path loss generally decays with respect to the distance. The empirical model giving a relationship between path loss and distance dependency is given by:

$$PL_{\mathrm{dB}} = PL_{\mathrm{dB}}(d_0) + 10n \log(d/d_0) + \delta_\sigma \qquad (2)$$

where $PL_{\mathrm{dB}}(d_0)$ is the average path loss at the reference distance $d_0 = 1$ m. is the path loss exponent. The lognormal shadow fading X_σ is a Gaussian random variable with zero-mean (in dB) and standard deviation also in (dB). Using a linear least mean square, $PL_{\mathrm{dB}}(d_0)$ and n are estimated. Fig. 4 and Fig. 5 illustrate the path loss as a function of the distance in LOS and NLOS, respectively. Table 1 gives the path
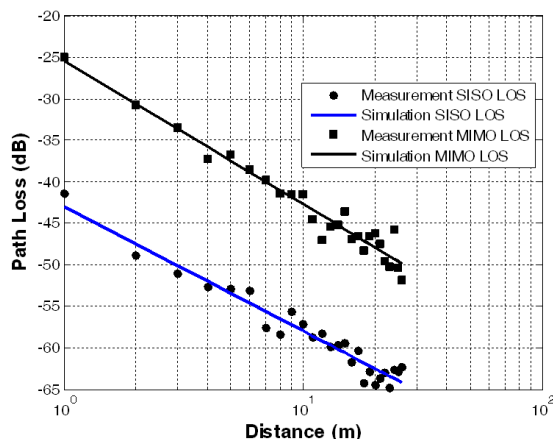
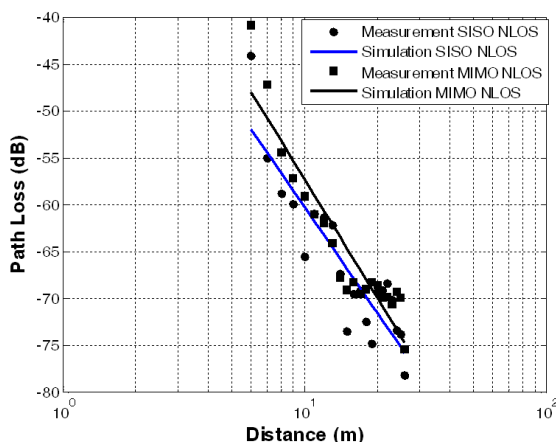**Figure 4.** Path loss versus distance in LOS scenario.

Figure 5. Path loss versus distance (dB) in NLOS scenario.

loss exponent and the standard deviation of the random variable in all four cases. In the LOS scenario, the path loss is much better than free space. In the LOS case, for MIMO and SISO, the values of n and σ are ($n = 1.76$, $\sigma = 1.16$ dB) and ($n = 1.50$, $\sigma = 3.24$ dB), respectively. And for the NLOS case, the values were ($n = 4.2$, $\sigma = 2.53$ dB) and ($n = 3.74$, $\sigma = 4.18$ dB), for MIMO and SISO, respectively. The path loss exponents are almost similar in both MIMO and SISO. Our results are compared to those obtained in the same mine, but in another gallery [3]. The obtained path loss exponent is around 2.03 at the

Table 1. Path loss exponent n and the standard deviation of the random variable σ (dB).

	MIMO		SISO	
	LOS	NLOS	LOS	NLOS
n	1.76	4.20	1.5	3.74
σ (dB)	1.16	2.53	3.24	4.18

same frequency of 2.45 GHz. In the NLOS situation, our value of 4.24 is much smaller compared to the value published by Bouttin et al. [3]. This is due of the difference in the dimensions of the gallery and the type of the antennas used in these measurements.

5. TIME PROPERTIES

In an undeground environment, multipath is very important due to the reflection and scattering from the ground and surrounding rough surfaces. Multiple paths come with various delays, causing inter symbol interference (ISI). ISI is the result of the overlapping of transmitted symbols at the receiving end of a communication system. Therefore, the maximum data rates on the communication applications could be limited by ISI. The power delay profiles (PDP) are derived from the frequency channel responses by using an inverse fast Fourier transform (IFFT) with a Hanning window function to reduce the side lobe level. An example of PDP for a MIMO in LOS situation at a distance of 2 m is shown on Fig. 6. From the impulse response graph, shown in Fig. 6, a strong path caused by the direct Line of sight (LOS) followed by a series of delayed paths exponentially decaying in power is noticed. Furthermore, the First-arrival delay is extracted and it equals to 6.98 ns for a distance of 2 m between the transmitter and receiver. An experimental distance of 2.09 m is then obtained. The delay spread is calculated from power delay profiles given by the square of magnitude of the channel impulse response. It is defined as [16]:

$$\tau_{\mathrm{rms}} = \sqrt{\bar{\tau^2} - \bar{\tau}^2} \tag{3}$$

$\bar{\tau}$, the first moment is defined as:

$$\bar{\tau} = \frac{\Sigma_k a_k^2 \cdot \tau_k}{\Sigma_k a_k^2} = \frac{\Sigma_k p(\tau_k) \cdot \tau_k}{\Sigma_k p(\tau_k)} \tag{4}$$

and

$$\bar{\tau}^2 = \frac{\Sigma_k a_k^2 \cdot \tau_k^2}{\Sigma_k a_k^2} = \frac{\Sigma_k p(\tau_k) \cdot \tau_k^2}{\Sigma_k p(\tau_k)} \tag{5}$$
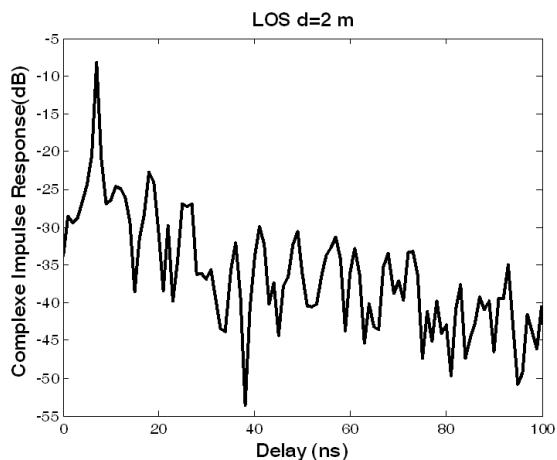
Figure 6. Example of power delay profile for MIMO at 2 m in LOS.

Table 2. Mean, Standard deviation, and Max of the RMS delay spread in ns for two thresholds.

	10 dB		15 dB	
All values in (ns)	MIMO	SISO	MIMO	SISO
Mean	1.78	4.88	3.23	8.44
Standard deviation	0.98	1.76	3.24	2.37
Max	3.81	8.54	7.75	13.47

where a_k, $p(\tau_k)$, and τ_k are the gain, power, and delay of the kth path, respectively.

In the LOS scenario, the delay were calculated by taking the multipath components with amplitudes within 10 dB and 15 dB, of the peak value of the PDF, for MIMO and SISO. The cumulative distribution function has been plotted in Fig. 7. The delay spread rms, for 50% of all locations is equal or less than 2 ns, and 3.5 ns for the threshold value of 10 and 15 dB in the case of the MIMO, respectively. However, in the SISO case τ_{rms} is less or equal to 4.5 ns and to 8 ns for the same threshold. The mean, maximum and the standard deviation of the delay spread are summarized in Table 2. It can be concluded that the delay spread increases when the threshold level increases. This is expected as there are more multipath components with an increase of the threshold level. It can also be noted that the delay spread is
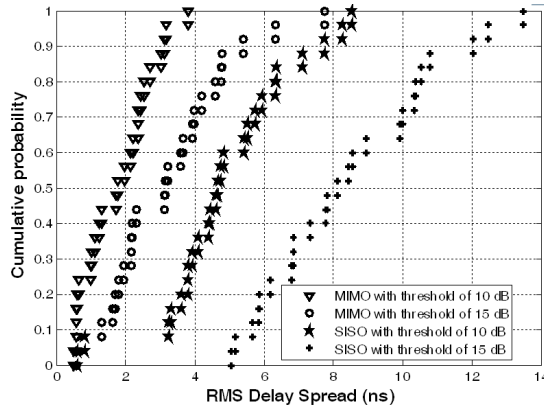
Figure 7. Cumulative distribution function for two thresholds for MIMO and SISO in LOS.

Table 3. Mean, standard deviation, maximum of τ_m and τ_{max} in ns at 2.4 GHz.

All values in (ns)	τ_m		τ_{max}	
	MIMO	SISO	MIMO	SISO
mean	46.21	45.08	59.31	77.19
Standard deviation	25.72	22.91	29.64	28.21
Max	90.99	84.61	107.98	125.98

smaller in the MIMO case, as shown in Fig. 8 with a threshold level of 15 dB. This is due to the fact that in the MIMO the LOS component is stronger than the SISO. The delay spread does not increase with the transceiver-receiver separation.

As explained by Sun and Akyildiz [17], the delay spread in an underground surroundings is influenced by the number of significant modes which exists and the transmitter receiver distance. The same conclusion on the propagation behavior in underground environments was obtained in [3, 4]. The mean excess delay and the maximum excess delay have also been computed for a threshold level of 15 dB. The different values are presented in Table 3. It can be seen that, for MIMO and SISO, that the mean excess delay varies from 13.41 ns to 91 ns and from 12.55 ns to 84.61 ns, respectively. The average values for MIMO and SISO are 46.21 ns and 45.08 ns, respectively. The maximum excess delay varies from 15.5 ns to 108 ns for MIMO and from 31.99 ns
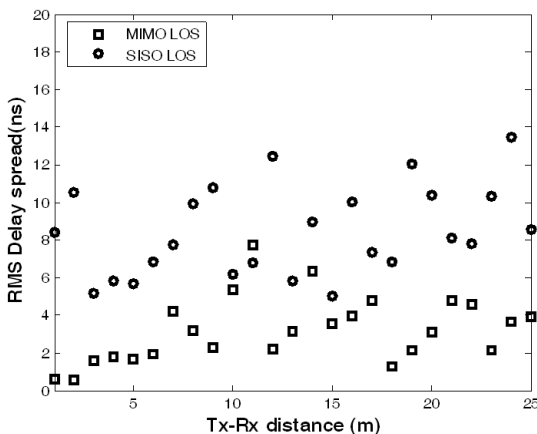
Figure 8. Comparison of the delay spread for MIMO and SISO for a threshold of 15 dB in LOS.
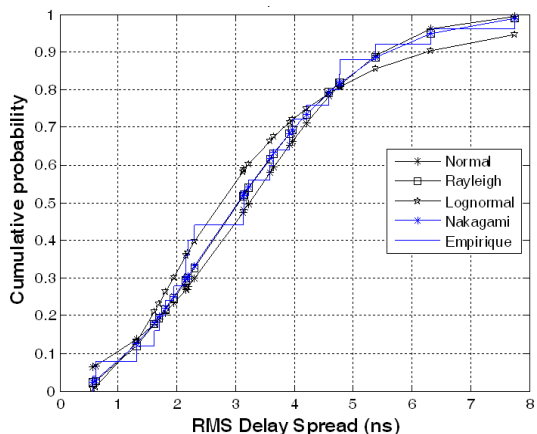

Figure 9. Cumulative distribution function of the RMS and different distributions.

to 126 ns for SISO. The average value for MIMO and SISO are 59.31 ns and 77.18 ns, respectively.

The cumulative distribution function of the delay spread for the MIMO in LOS with a threshold of 15 dB has been plotted in Fig. 9. This measured data is fitted to a normal, lognormal, Raleigh, and Nakagami distributions in order to find the one which represents the best the measured data. The Aikake Information Criterion (AIC) test

was used. The AIC is defined as [18–21]:

$$AIC = 2q + k \ln \left(\frac{\sum\limits_{i=1}^{n} (y_i - f(x_i))^2}{k} \right) \tag{6}$$

where q, k, y_i and $f(x_i)$ are the number of parameter in the statistical model, the number of samples in the measured data, the measured data and the probability density function of the statistical model, power and delay of the kth path, respectively. Fig. 9 shows the CDF of the measured with the fitted distribution function. The lognormal distribution, which has the lowest AIC, is the best fit for the measured data.

6. CHANNEL CAPACITY

The channel capacity is defined as the highest transfer rate of information, which is allowed to be transmitted with a low arbitrary error probability [7]. For MIMO systems, the system capacity depends highly on the statistical properties of the channel matrix. In fact, under a flat fading channel, and for a fixed transmitted power configured at $10\,\mathrm{dBm}$ and a noise floor of $-110\,\mathrm{dBm}$, with no channel state information (CSI) at the receiver, the M^*N MIMO channel capacity can be expressed by (7), assuming the transmitted power to be uniformly distributed among the N receiving antennas [22].

$$C = \log_2 \left(\det \left[I_M + \frac{\sigma}{N} H H^* \right] \right) \frac{\text{bits}}{\frac{\text{s}}{\text{Hz}}} \tag{7}$$

Where I_M is the M^*M identity matrix, σ the average SNR per receive antenna, H the channel matrix, and * the complex conjugate transpose. Equation (7) is only applied when $M < N$. If $M > N$, the term HH^* is replaced by H^*H, and I_M is replaced by I_N. In addition, for a frequency selective channel, the MIMO channel capacity is obtained through an average over the whole bandwidth [23].

$$C_f = \in_f \left\langle \log_2 \left(\det \left[I_M + \frac{\sigma}{N} H H^* \right] \right) \right\rangle \frac{\text{bits}}{\frac{\text{s}}{\text{Hz}}} \tag{8}$$

Where $\in_f$ refers to the mathematical expectation over the channel bandwidth. Indeed, in our study, the measured spectrum (BW = $100\,\mathrm{MHz}$, between $2.4\,\mathrm{GHz}$ and $2.5\,\mathrm{GHz}$) is subdivided in several sub bands, each of length $\Delta_f = 156\,\mathrm{kHz}$. then, the channel capacities for the SISO and 2×2 MIMO system are calculated for each sub band assuming a fixed SNR of $10\,\mathrm{dB}$ at the receiver, and then

averaged over the 100 MHz bandwidth. The relationship between the average channel capacity for both MIMO and SISO scenarios, and the distance between the transmitter and the receiver is given by Fig. 10.
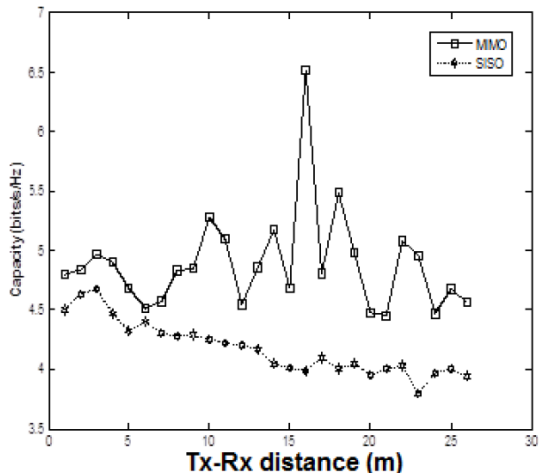

Figure 10. Comparison of the capacity for MIMO and SISO in LOS condition.

As expected, there is a clear gain in capacity with the MIMO configuration over the classical SISO system. In fact, it is observed from the figure above, that capacity in the MIMO scheme is almost all greater than the one in the SISO scheme. Hence, this confirms the fact that using more antenna elements provides an increase in terms of channel capacity.

7. CONCLUSION

In this paper, a MIMO channel propagation has been studied in an underground mine at the frequency of 2.45 GHz. Different statistical parameters have been presented. For comparison reasons, a SISO channel has also been characterized.

Monopole antennas with a spatial distance of $\lambda/2$ at the frequency of the 2.45 GHz have been used as transmitting and receiving antennas in the 2×2 MIMO. The results show that the path loss exponent is less than 2 in the LOS scenario for MIMO and SISO, however for NLOS the path loss exponent is around 4. The multipath nature of the real underground mine has shown by the value of the path loss exponent, which is less than the one of free space in LOS. It has also been demonstrated that the RMS delay spread is not correlated to the

distance because of multimodes nature of the underground mine. The RMS delay spread in the MIMO channel is less than the SISO case in LOS. This is can be explained by the strong LOS component present in the MIMO.

The delay spread varies between 3 ns and 7.75 ns with a mean value of 3.24 ns for the MIMO LOS with a threshold of 15 dB. The lognormal distribution represents best the RMS delay spread. For a constant SNR, higher capacities are obtained with the MIMO channel compared to the SISO. The capacity in MIMO is clearly enhanced. Therefore, with such performances, MIMO can be used in in mining industry to improve the different communication systems. These systems can improve the security and the productivity and also help to communicate with miners in the case of a disaster.

ACKNOWLEDGMENT

REFERENCES

1. Outalha, S., R. Le, and P. M. Tardif, " Toward a unified and digital communication system for underground mines," *Revue of Canadian Institute of Mining, Metallurgy and Petroleum*, Vol. 93, No. 1044, 100–105, 2000.

2. Nedil, M., A. M. Habib, A. Djaiz, and T. A. Denidni, " Design of new mm-Wave Antenna fed by CPW Inductively Coupling fo mining communication," *IEEE Antenna and Propagation Society*, 1–4, Jun. 2009.

3. Boutin, M., A. Benzakour, C. Despins, and S. Affes " Radio wave characterization and modeling in underground mine tunnels," *IEEE Trans. on Antennas and Propag.*, Vol. 56, No. 2, 540–549, Feb. 2008.

4. Nerguizian, C., C. Despins, S. Affes, and M. Djadel, "Radio-channel characterization of an underground mine at 2.4 GHz," *IEEE Transactions on Wireless Communications*, Vol. 4, No. 5, 2441–2453, Sept. 2005.

5. Molisch, A. F., M. Steinbauer, M. Toeltsch, E. Bonek, and R. Thoma, "Capacity of MIMO systems based on measured wireless channels," *IEEE J. Sel. Areas Commun.*, Vol. 20, 561–569, 2002.

6. Foschini, G. J. and M. J. Gans, " On limit of wireless communications in a fading environment when using multiple antennas," *Wireless Personal Commun.*, Vol. 6, No. 3, 315–335, Mar. 1996.

7. Telatar, I. E., "Capacity of multi-antenna Gaussian channels," *Eur. Trans. Telecommun.*, Vol. 10, No. 6, 585–595, 1999.

8. Molina-Garcia-Pardo, J. M., J. V. Rodriguez, and L. J. Llacer, "Polarized indoor MIMO channel measurements at 2.45 GHz," *IEEE Trans. on Antennas and Propag.*, Vol. 56, No. 12, 3818–3828, Dec. 2008.

9. Jaramillo, R. E., O. Fernandez, and R. P. Torres," Empirical analysis of 2×2 MIMO channel in outdoor-indoor scenarios for BFWA applications," *IEEE Antennas and Propagation Magazine*, Vol. 48, No. 6, Dec. 2006.

10. Donlan, B. M., D. R. McKinstry, and R. M. Buehrer, " The UWB indoor channel: Large and small scale modeling," *IEEE J. Sel. Areas Commun.*, Vol. 5, No. 10, 2863–2873, 2006.

11. Valdesueiro, J. A., B. Izquierdo, and J. Romeu," On 2×2 MIMO observable capacity in subway tunnels at C-band: An experimental approach," *Antennas and Wireless Propagation Letters*, Vol. 9, 1099–1102, Dec. 2006.

12. Sun, Z. and I. F. Akyildiz, "Optimal MIMO antenna geometry analysis for wireless networks in underground tunnels," *Global Telecommun. Conf.*, Vol. 9, 1–6, 2009.

13. Lienard, M., P. Degauque, J. Baudet, and D. Degardin, "Investigation on MIMO channels in subway tunnels," *IEEE J. Sel. Areas Commun.*, Vol. 21, No. 3, 332–339, Apr. 2003.

14. Molina-Garcia-Pardo, J. M., M. Lienard, P. Degauque, D. G. Dudley, and L. Juan-Llacer. "Interpretation of MIMO channel characteristics in rectangular tunnels from modal theory," *IEEE Transactions on Vehicular Technology*, Vol. 57, No. 3, 1974–1979, Apr. 2003.

15. Molina-Garcia-Pardo, J. M., M. Lienard, P. Degauque, C. Molina-Garcia-Pardo, and L. J. Llacer, "MIMO channel capacity with polarization diversity in arched tunnels," *Antennas and Wireless Propagation Letters*, Vol. 8, No. 3, 1186–1189, 2009.

16. Rappaport, T. S., *Wireless Communications: Principle and Practice*, Prentice-Hall, Englewood Cliffs, NJ, 1999.

17. Sun, Z. and I. F. Akyildiz, "Channel modeling and analysis for wireless networks in underground mines and road tunnels," *IEEE Transactions on Communicat.*, Vol. 58, No. 6, 1758–1768,

Jun. 2010.

18. Akaike, H., "A new look at the statistical model identification," *IEEE Trans. Automat. Control*, Vol. 19, No. 6, 716–723, Dec. 1974.

19. Lustmann, Y. and D. Porrat, "Polarized indoor MIMO channel measurements at 2.45 GHz," *IEEE Trans. on Antennas and Propag.*, Vol. 58, No. 11, 3685–3692, Nov. 2010.

20. Schuster, U. G. and H. Bolcskei, " Ultrawideband channel modeling on the basis of information-theoretic criteria," *IEEE Transactions on Wireless Communications*, Vol. 6, No. 7, 2464–2475, Jul. 2007.

21. Sani, A., A. Alomainy, G. Palikaras, Y. Nechayev, Y. Hao, C. Parini, and P. S. Hall, " Experimental characterization of UWB on-body radio channel in indoor environment considering different antennas," *IEEE Trans. on Antennas and Propag.*, Vol. 58, No. 1, 238–241, Jan. 2010.

22. Mtumbuka, M. C. and D. J. Edwards, "Investigation of tri-polarised MIMO technique," *Electron. Lett.*, Vol. 41, No. 3, 137–138, Feb. 2005.

23. Mtumbuka, M., W. Q. Malik, C. J. Stevens, and D. J. Edwards, " A tri-polarized ultra-wideband MIMO system," *Proc. IEEE Sarnoff Symposium on Advances in Wired and Wireless Communications*, Princeton, NJ, 98–101, Apr. 2005.